CHAPTER V
POROUS STRUCTURE OF POLYBENZOXAZINE-BASED ORGANIC AEROGEL PREPARED BY SOL-GEL PROCESS AND THEIR CARBON AEROGELS

5.1 Abstract

New organic aerogels were successfully prepared from a new class of phenolic resins called polybenzoxazines synthesized via conventional thermal curing reaction of a benzoxazine monomer using xylene as a solvent. Without the need for using supercritical conditions to remove the solvent during the process, the carbon aerogels were obtained with a much shortened time. From two different concentrations of benzoxazine solution, 20 and 40 wt%, the resulting polybenzoxazine aerogels, having densities of 260 and 590 kg/m^3, respectively, were obtained after the curing process. The subsequent carbon aerogels were prepared by the carbonization of polybenzoxazine aerogels. The corresponding carbon aerogels exhibited a microporous structure with pore diameters less than 2 nm, the densities of 300 and 830 kg/m^3, and surface areas of 384 and 391 m^2/g, respectively. The texture of the carbon aerogels was denser than that of their organic aerogel precursor, as evidenced by scanning electron microscopy. The transformation of the polybenzoxazine aerogel to the carbon aerogel was clearly observed using fourier transform infrared spectroscopy.

(Key-word: Benzoxazine; Aerogel; Carbon aerogel; Microporous)

5.2 Introduction

Aerogel is a microporous material which consists of many contiguous micropores. The morphology of aerogel can be modified by using different synthesis parameters. This characteristic makes the aerogel particularly well adapted for various applications such as fuel cells, host material of catalysts, thermal insulators, and molecular sieves. Carbon aerogel, a novel form of aerogels, was first produced by Pekala *et al.* [1]. Organic aerogel and carbon aerogel processing have been widely developed to simplify the process. The traditional process for organic aerogel preparation is typical via the sol–gel polymerization of an organic solution followed by supercritical drying of the attained hydrogel to extract the solvent in the gel structure; and then the obtained organic aerogel is transformed into carbon aerogel via pyrolysis [1]. The total process of carbon aerogel preparation requires approximately 2 weeks. Recently, many attempts have been made to shorten the process, such as using alcohol-sol–gel polymerization and drying with supercritical acetone to avoid the solvent exchanging period [2]. The organic and carbon aeorgel processing normally uses resorcinol (R) and formaldehyde (F) as the precursor. The RF aerogels consist of a highly crosslinked aromatic polymer. In order to obtain carbon aerogel, the RF gel is carbonized in an inert atmosphere. Basically, the crosslink density of organic gel is a key parameter that needs to be considered for aerogel applications. Highly crosslinked organic gel not only provides high structural stability in order to preserve its structure after solvent removal, but also introduces high char yield after pyrolysis to construct the carbon aerogel. In order to find a reactant to synthesize the organic aerogel and transform it to carbon aerogel, these two characteristics of the synthesized gel need to be considered. A new class of phenolic resin, namely polybenzoxazine, was recently developed. Polybenzoxazine has excellent molecular design flexibility that allows the properties of the cured materials to be controlled for various applications. Furthermore, polybenzoxazine has many advantageous characteristics compared with traditional phenolic resin, such as high thermal stability and excellent mechanical properties, easy processibility, low water absorption, and near zero shrinkage after polymerization [3–5]. According to Ishida [6], the synthesis of the benzoxazine monomers consists of a few simple steps

using the patented solventless synthesis technique. As benzoxazine resin can be cured through thermally activated ring-opening polymerization without a catalyst, and its mechanical properties can rapidly develop even at low crosslinking conversion, polybenzoxazine becomes an excellent candidate resin to replace the traditional reactant for organic and carbon aerogel preparations. Moreover, the thermal and thermooxidative resistance can be improved by enhancing its crosslink density, which results in high char yield and low flammability, [7].

The polybenzoxazine (Ba-A) used in this study is based on bisphenol A and aniline, which is one of the very first polybenzoxazines synthesized [8]. Ba-A can maintain its mechanical integrity up to 165 °C, which is its glass transition temperature. The decomposition temperature at 5% weight loss is approximately 370°–380 °C and the char yield of the reported benzoxazine at 800 °C is around 30% weight [8]. These characteristics enable Ba-A to be an appropriate reactant for carbon aerogel.

5.3 Experimental

5.3.1 Materials

The materials used in this research were benzoxazine resin with xylene as a solvent. This benzoxazine resin is based on bisphenol-A, aniline and formaldehyde. Commercial grade bisphenol-A was kindly provided by Bayer Thai Co., Ltd. Para-formaldehyde (95%) was purchased from BDH Laboratory Supplies and aniline (99%) was purchased from Panreac Quimica SA Company. The solvent, xylene (98%), was obtained from Carlo Erba Reagenti.

5.3.2 Oragnic and Carbon Aerogel Preparation

A benzoxazine monomer was synthesized via the solventless process proposed by Ishida *et al.* [6]. Bisphenol A, aniline, and paraformaldehyde, at a 1:2:4 molar ratio, were mixed together and heated at 110 °C for 60 min until the mixture became a transparent pale yellow color. The monomer was used without further purification. The precursors and the synthetic reaction of polybenzoxazine are shown

in Scheme 5.1. Benzoxazine solutions were prepared from the benzoxazine monomer using xylene as a solvent. The monomer concentrations were kept at 20 and 40 wt%. After that, the mixtures were transferred into vials and sealed. The temperature was slowly raised to 130 °C for 96 h in an oven. The attained products were partially cured benzoxazine hydrogels. The organic aerogels were then obtained by drying the hydrogels at ambient temperature and pressure for 2 days to remove the xylene from their matrices. The aerogels were step-cured in an oven at 160°, 180 °C for an hour at each temperature and 200 °C for 2 h. The specimens were finally left to cool to room temperature and were then ready for further characterization. After step-curing, the carbon aerogels were prepared by the pyrolysis of the organic aerogels in a quartz reactor. The pyrolysis took place in a tube furnace under nitrogen flow at 500 cm^3/min using the following ramp cycle from: 30° to 250 °C for 60 min, 250° to 600 °C for 300 min, 600° to 800 °C for 60 min and held at 800 C for 60 min. Then the furnace was cooled to room temperature under nitrogen atmosphere. Here, the organic aerogel and the carbon aerogel were denoted as BA-xx % and CA-xx %, respectively, where the xx denotes the monomer solution concentration of xx wt%.

5.3.3 Characterization of The Organic and Carbon Aerogels

Aerogel density was determined by weighing the spherically shaped aerogel and dividing the weight by the measured volume. A PerkinElmer differential scanning calorimeter, DSC 7, was used to study the curing behavior of the polybenzoxazine and polybenzoxazine aerogel. Approximately 5–9 mg samples were sealed in aluminum pans and analyzed using temperature ramp rates of 1 and 10 C/min under nitrogen atmosphere. The microstructure of the organic and carbon aerogels was observed by scanning electron microscopy (SEM) using a JEOL-JSM 5800LV at an acceleration voltage of 15 kV. The samples were coated with gold and then the microstructure images of the samples were recorded. The IR spectra of the samples were recorded by a Thermo Nicolet Nexus 670 FT-IR analyzer. The samples were ground and mixed with KBr powder and then pressed into a pellet. The porous structure of the carbon aerogels was measured by the nitrogen adsorption method in order to acquire the surface area, pore volume, pore size, and pore size distribution of

the samples. Before each adsorption test, the carbon aerogels were degassed at 300 °C to remove all volatile adsorbed species. Nitrogen adsorption–desorption isotherms were measured using a Quantachrome-Autosorb-1. BET surface area (S_{BET}) was calculated by applying the BET (Brunauer–Emmett–Teller) theory. The calculated micropore volume (V_{mic}) and micropore surface area (S_{mic}) could be obtained by using the t-plot method with respect to a difference in capability to form multilayer adsorption between micropore and larger pores, i.e., mesopore, macropore and outside surface. Mesopore volume (V_{mes}) and mesopore surface area (S_{mes}) were calculated using the BJH (Barrett– Johner–Halendar) theory, in which the pore size was calculated from the Kelvin equation and the selected statistical thickness equation [9–12]. A PerkinElmer TG/DTA thermogravimetric analyzer, model SII Diamond, was used to examine the decomposition temperature and char yield of the polybenzoxazine. Approximate 20 mg of the polybenzoxazine was heated from 30° to 900 °C using a heating rate of 20 °C/min under nitrogen atmosphere. The microstructure surface of the obtained aerogel was investigated using H-7650 Hitachi High-Technologies transmission electron microscope (TEM) system. The carbon aerogel was ground and dispersed with distilled water before placing it on a copper grid and analyzing it at 100 kV.

5.4 Results and Discussion

The investigation of the static pre-curing temperature of the benzoxazine resin was accomplished by using DSC with a relatively slow heating rate of 1 °C/min. Figure 5.1 shows the DSC thermogram of curing exothermic peak of the benzoxazine monomer. As seen from this figure, the exothermic peak of the monomer, corresponding to its ring opening polymerization, was located at 120°–240 °C. In order to clarify the appropriate pre-curing temperature, both the pre-curing temperature of the resin and the boiling temperature of the solvent have to be considered. Based on the DSC result, a pre-curing temperature of 130 °C was used in this study because it can produce the polymerization reaction of benzoxazine without boiling the xylene (135 °C). The TGA thermogram of the polybenzoxazine is

presented in Figure 5.2. It began to lose weight at 250 °C, and the highest maximum mass loss rate was observed in the temperature range of 250°–600 °C, which was caused by the production of a large amount of volatile materials. The rate of mass loss became slower after 600 °C and an obvious mass loss could not be observed beyond 800 °C. According to this TGA thermogram, the carbon aerogels were prepared by the pyrolysis of organic aerogels following the three ramp cycles from: 30° to 250 °C, 250° to 600 °C, and 600° to 800 °C. Moreover, from the thermogram, it can be seen that the degradation temperature at 5% weight loss and the char yield at 800 °C of the synthesized polybenzoxazine was 330 °C and 25 wt%, respectively. Kasinee *et al.* [8] identified the decomposition products of aromatic amine-based polybenzoxazines through TGA and GC-MS techniques. They found that the decomposition products were a combination of benzene derivatives, amines, phenolic compounds, and Mannich base compounds.

Figure 5.3 shows the IR spectra of the benzoxazine monomer and uncured polybenzoxazine aerogels. The characteristic absorption bands of the benzoxazine monomer structure (Figure 5.3a) appeared at 1230–1236 cm^{-1} and 1028–1036 cm^{-1} (symmetric stretching of C–O–C), and 920–950 cm^{-1} and 1491–1500 cm^{-1} (tri-substituted benzene ring) [13]. Compared with the spectra of uncured polybenzoxazine (Figure 5.3b, c), there was an obvious change of the characteristic absorption band in the region of 920–950 cm^{-1}. As seen in the figure, the absorption band significantly decreased after the pre-curing benzoxazine solutions at 130 °C for 96 h. This FTIR result strongly agrees with the study of Takeichi *et al.* [14], which suggested that the characteristic absorption change was due to the ring-opening polymerization of the benzoxazine resin. The influence of the solution concentration was also observed in this experiment. The intensity of the absorption band decreased more significantly when the concentration was increased from 20 to 40 wt%. According to this result, it can be inferred that the concentration of the benzoxazine solution affected the conversion of the curing reaction, which will be further investigated. Additionally, the existence of this absorption band of the aerogels could imply that these aerogels could not be completely cured at 130 °C, even for a long time. Benzoxazine resin was proposed to thermally polymerize through ring-opening

polymerization by heating without a catalyst or an initiator [15], the convenient thermal step cure was employed in this study. In order to investigate the curing behaviors of the polybenzoxazine and polybenzoxazine aerogel, DSC was used with a heating rate of 10 °C/min. The thermograms of the curing exothermic peak of benzoxazine monomer and polybenzoxazine aerogels are shown in Figure 5.4. The thermogram of the benzoxazine monomer revealed the exotherm in the temperature range of 180°–280 °C, representing its curing reaction [16]. The degree of curing conversion of the samples was determined from the ratio between the remaining heat of reaction of the polybenzoxazine aerogels and the heat of reaction of the benzoxazine monomer. The heat of reaction determined from the area under the exothermic peak was 262.68 J/g for the benzoxazine monomer. After the proposed step cure, the area was reduced to 42.31 and 59.51 J/g of polybenzoxazine aerogels from the solution with concentrations of 20 and 40 wt%, corresponding to 77 and 84% curing conversion of the aerogels, respectively. The obtained curing conversion indicated that the curing reaction of the benzoxazine solution with higher concentration could perform more efficiently at the same curing conditions. Furthermore, as clearly seen in this figure, the exothermic peaks at around 180°–300 °C of the aerogels which were step cured disappeared. This evidence could imply that the curing reaction of polybenzoxazine aerogels became practically complete. Figure 5.5 shows the FTIR spectra of the benzoxazine monomer, the fully cured polybenzoxazine, as identified by the DSC in Figure 5.4, the fully cured polybenzoxazine aerogel, and the carbon aerogel. In contrast with the IR spectra of the benzoxazine monomer, the characteristic absorption band, due to the tri-substituted benzene ring at 920–950 cm^{-1} of the fully cured polybenzoxazine aerogels, almost disappeared. This indicated that the resulting organic aerogel could be completely cured by using this proposed step curing method. This FTIR spectrum gave a result consistent with the previous DCS results. Due to the similar appearance of the fully cured polybenzoxazine and fully cured polybenzoxazine aerogel absorption bands, it could be inferred that after the ambient drying and curing process, there was no detectable amount of xylene remaining in the resulting aerogel, although the drying period was only a couple of days. Moreover, the spectrum could

confirm that a chemical interaction between the polybenzoxazine and the xylene did not exist during this process. From the spectra of fully cured polybenzoxazine aerogels (Figure 5.5c, d) and carbon aerogel (Figure 5.5e), the obvious changes in absorbance due to chemical transformations from the polybenzoxazine organic aerogel to carbon aerogel could be easily observed. After the organic aerogels were carbonized at 800 C, the characteristic absorption bands of the organic compound were no longer seen. This result strongly agrees with the study of Li *et al.* [17] which investigated the chemical and physical changes during the pyrolysis process of cresol–formaldehyde. They observed that the intensity of the organic absorption peaks becomes weaker with an increase of pyrolysis temperature, and the absorption peaks almost completely disappear at 800 °C. They also suggested that the aromatic rings rearrange themselves, leading to bound carbon rings during the pyrolysis.

Scanning electron microscopy with a magnification of 5,000 was employed to investigate the macrostructure of the materials. Figure 5.6 shows images of the fully cured polybenzoxazine, fully cured polybenzoxazine aerogels, and their carbonized products. The polybenzoxazine and carbon aerogels prepared from BA-20% were composed of agglomerated polybenzoxazine or carbon particles in three dimensions with contiguous open macropores analogous to that of the typical RF aerogels prepared by R. Petricevic *et al.* and Shen *et al.* [18, 19]. For the organic and carbon aerogels from BA-40%, the solid phase exhibits a smooth continuous polymer network incorporated with open macropores, which can be clearly seen in Figure 5.6e and f. In addition, the carbon aerogels revealed a denser porous structure corresponding to their densities, which will be further discussed. Since aerogel is a porous solid material which is composed of contiguous open macropores in combination with many ultra fine micropores, its density and surface area are important indices to judge its quality. The measured density and pore texture of polybenzoxazine, polybenzoxazine aerogels and carbon aerogels are listed in Table 5.1. An increase in the concentration of the monomer solution led to an increase in the density of the resulting solid, which in turn resulted in a decrease of the vacancies within the solid skeleton when the solvent was removed. This result strongly agrees with the SEM study previously discussed. In addition, the density of the carbon aerogels was greater than that of their precursory organic aerogels, which could

generally be seen in the carbonization of other organic aerogels. This phenomenon was also observed by other related works. Shen *et al.* and Wu *et al.* [10, 19] found that the bulk density and gelation ability of organic and carbon aerogels increased with increasing resorcinol-formaldehyde (RF) and phenol-furfural (PF) concentration, and they also found that the density of the materials increased after the transformation of organic to carbon aerogel.

According to the nitrogen adsorption measurement classified by IUPAC, the common factors affecting the adsorption isotherms are the characteristics of the adsorbent and the interaction between the adsorbate and the adsorbent. In our case, the materials are classified as Type I, which is divided into Type Ia–c isotherms, depending on the pore-size distribution of materials. Type Ia corresponds to materials having quite narrow micropore, Type Ib corresponds to materials having wider micropore than Type Ia, and Type Ic corresponds to materials having mesopores together with micropore [20]. The adsorption–desorption isotherms of nitrogen on carbon aerogels at 77 K are shown in Figure 5.7. The amount of nitrogen adsorbed and desorbed was plotted against the relative pressure. According to the IUPAC classification, both isotherms of the carbon aerogels were Type Ib, characteristic of microporous adsorbents [20, 21]. Moreover, the isotherm of ideal Type I microporous material is concave to the P/Po axis with asymptotic approach to a limited value of adsorption; as a result a hysteresis loop should not be observed. The Type I isotherm is principally observed when molecular adsorption is limited to only a few layers. However, for materials having a wide range of pore sizes, the adsorption–desorption isotherms could be a combination of isotherms, which deviate from the ideal isotherm [9]. When considering the isotherms of the carbon aerogels, the isotherms trivially deviate from the ideal Type-I isotherm. As also observed by Shen *et al.* [19] the deviation corresponds to multilayer adsorption and capillary condensation occur on the sorbent surface if the pore size is smaller than 2–3 nm. In order to acquire an equitable comparison between the pore textures of the resulting carbon aerogels in this research and those of the reference carbon aerogels from other organic precursors, the same calculation method for each parameter should be applied. The BET surface area was calculated using the BET theory. Micropore volume and micropore surface area were calculated using the t-plot theory. Mesopore

volume and mesopore surface area were calculated using the BJH theory [10–12]. The calculated parameters of the resulting carbon aerogels compared with those of the other organic precursors are shown in Table 5.1 and 5.2. The data in Table 5.1 shows that the polybenzoxazine derived carbon aerogels have a high surface area (384 and 391 m^2/g) with relatively large pore volume (0.21 cm^3/g). The average pore diameter of the aerogels is 2 nm, which is in the micropore range. This result agrees very well with the adsorption isotherm classification. According to the pore size distribution (Figure 5.8), the pore diameters of the carbon aerogels are less than 10 nm. The effects of the monomer solution concentration and the characteristics of the porosity of the carbon aerogels can be deduced from Table 5.2. We found that when the concentration of the monomer solution was increased, the BET surface area of the derived carbon aerogel increased. However, the concentration does not have a significant effect on the other porous characteristics, including pore size, pore volume, and pore size distribution. When considering the micropore and mesopore portions of the areogels, the most prominent characteristic of the polybenzoxazine-derived carbon aerogels is high proportion of micropore volume to micropore surface area, as compared with organic aerogels obtained from other precursors, as can be seen in Table 5.2 [10–12]. From this microstructure investigation, it could be concluded that the concentration of the benzoxazine monomer solution slightly affects on the microstructure of the resulting aerogel, which consequently affects the macrostructure of the aerogels. By applying the mercury porosimetry (MP) method, the pore size distribution of the carbon aerogels was clearly seen. The pore size distribution of the carbon aerogel (Figure 5.8) is lower than 2 nm, implying that the resulting carbon aerogels can be classified as microporous materials. The TEM micrograph of the carbon aerogels obtained from BA-40% is shown in Figure 5.9. The ground carbon aerogel has a spherical shape with a porous structure. The pore size is less than 10 nm, which is in agreement with the result obtained from nitrogen adsorption analysis.

5.5 Conclusions

Polybenzoxazine organic aerogels and their related carbon aerogels have been successfully prepared by sol–gel process using xylene as a solvent. Since organic aerogels could be obtained directly from drying polybenzoxazine hydrogels at ambient conditions, the solvent exchange and supercritical drying process were eliminated. With this new approach of carbon aerogel fabrication, the total processing period was shortened from normally 2 weeks for RF to only 1 week for polybenzoxazine. The resulting organic and carbon aerogels comprise of three-dimensional contiguous open macropores containing a large number of micropores in their structures. Since the carbon aerogels consisted of numerous pores with sizes mainly lower than 2 nm, the aerogels could be classified as microporous materials. When considering the micropore and mesopore portions of the resulting areogels, these carbon aerogel structures had a higher proportion of micropore to mesopores, compared with carbon aerogels with the same density derived from other precursors or process which is the advantage of our materials. The experimental results showed that increase of the monomer solution concentration led to not only increase the bulk density but also increase BET surface area of the resulting polybenzoxazine and carbon aerogels.

5.6 Acknowledgments

This research is financially supported by the Thailand Research Fund (TRF), the Postgraduate Education and Research Program in Petroleum and Petrochemical Technology (ADB) Fund (Thailand), and the Ratchadapisake Sompote Fund, Chulalongkorn University. Additionally, the authors would like to thank Bayer Co., Ltd for their kind bisphenol-A support, and Mr. Robert Wright, our native English teacher/staff, for proof-reading this manuscript.

5.7 References

1. Pekala, R.W. (1989) Organic aerogels from the polycondensation of resorcinol. Journal of Materials Science, 24, 3221-3227.
2. Qin, G. and Guo, S. (2001) Preparation of RF organic aerogels and carbon aerogels by alcoholic sol–gel process. Carbon, 39, 1935-1937.
3. Ning, X. and Ishida, H. (1994) Phenolic materials via ring-opening polymerization: Synthesis and characterization of bisphenol-A based benzoxazines and their polymers. Journal of Polymer Science-Polymer Chemistry Edition, 32, 1121-1129.
4. Ning, X. and Ishida, H. (1994) Phenolic materials via ring-opening polymerization of benzoxazines: Effect of molecular structure on mechanical and dynamic mechanical properties. Journal of Polymer Science Polymer Physics Edition, 32, 921-927.
5. Ishida, H. and Allen D. (1996) Mechanical Characterization of Copolymers based on Benzoxazine and Epoxy. Polymer, 37, 4487-4495.
6. Ishida, H. (1996) U.S. Patent 5 543 516.
7. Brunovska, Z., Liu, J., and Ishida, H. (1999) 1,3,5-Triphenylhexahydro-1,3,5-triazine - active intermediate and precursor in the novel synthesis of benzoxazine monomers and oligomers. Macromolecular Chemistry and Physics, 200, 1745-1752.
8. Hemvichian, K. and Ishida, H. (2002) Thermal decomposition processes in aromatic amine-based polybenzoxazines investigated by TGA and GC–MS. Polymer, 43, 4391-4402.
9. Lowell, S., Shields, J.E., Thomas, M.A., and Thommes, M. (2004) Characterization of porous solids and powders: surface area, pore size, and density. New York.
10. Wu, D. and Fu, R. (2005) Fabrication and Physical Properties of Organic and Carbon Aerogel Derived from Phenol and Furfural. Journal of Porous Materials, 12, 311-316.

11. Wu, D. and Fu, R. (2006) Synthesis of organic and carbon aerogels from phenol-furfural by two-step polymerization. Microporous and Mesoporous Materials, 96, 115-120.

12. Wu, D., Fu, R., and Yu, Z. (2005) Organic and carbon aerogels from the NaOH-catalyzed polycondensation of resorcinol-furfural and supercritical drying in ethanol. Journal of Applied Polymer Science, 96, 1429-1435.

13. Agag, T. and Takeichi, T. (2003) Synthesis and Characterization of Novel Benzoxazine Monomers Containing Allyl Groups and Their High Performance Thermosets. Macromolecule, 36, 6010-6017.

14. Takeichi, T., Guoa, Y., and Rimdusit, S. (2005) Performance improvement of polybenzoxazine by alloying with polyimide: effect of preparation method on the properties. Polymer, 46, 4909-4916.

15. Su, Y.C., Chen, W.C., and Chang, F.C. (2004) Investigation of the thermal properties of novel adamantane-modified polybenzoxazine. Journal of Applied Polymer Science, 94, 932-940.

16. Ishida, H. and Sanders, D.P. (2000) Regioselectivity and Network Structure of Difunctional Alkyl-Substituted Aromatic Amine-Based Polybenzoxazines. Macromolecules, 33,8149-8157.

17. Li, W.C., Lu, A.H., and Guo, S.C. (2001) Characterization of the microstructures of organic and carbon aerogels based upon mixed cresol-formaldehyde. Carbon, 39, 1989-1994.

18. Petricevic, R., Glora, M., and Fricke, J. (2001) Planar Fibre Reinforced Carbon Aerogels for Application in PEM Fuel Cells. Carbon, 39, 857-867.

19. Shen, J., Hou, J., Guo, Y., Xue, H., Wu, G., and Zhou, B. (2005) Microstructure Control of RF and Carbon Aerogels Prepared by Sol-Gel Process. Journal of Sol-Gel Science and Technology, 36, 131-136.

20. Guzel, F., and Uzun, I. (2002) Determination of the Micropore Structures of Activated Carbons by Adsorption of Various Dyestuffs from Aqueous Solution. Turkish Journal of Chemistry, 26, 369-377.

21. Aranovich, G. and Donohue, M. (1998) Analysis of Adsorption Isotherms: Lattice Theory Predictions, Classification of Isotherms for Gas-Solid Equilibria, and Similarities in Gas and Liquid Adsorption Behavior. Journal of Colloid and Interface Science, 200, 273-290.

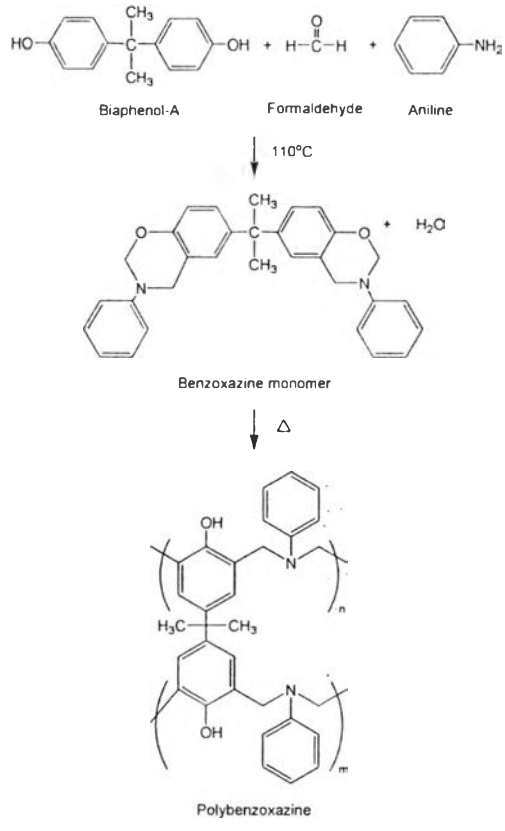

Scheme 5.1 The precursors and polybenzoxazine synthetic reaction.

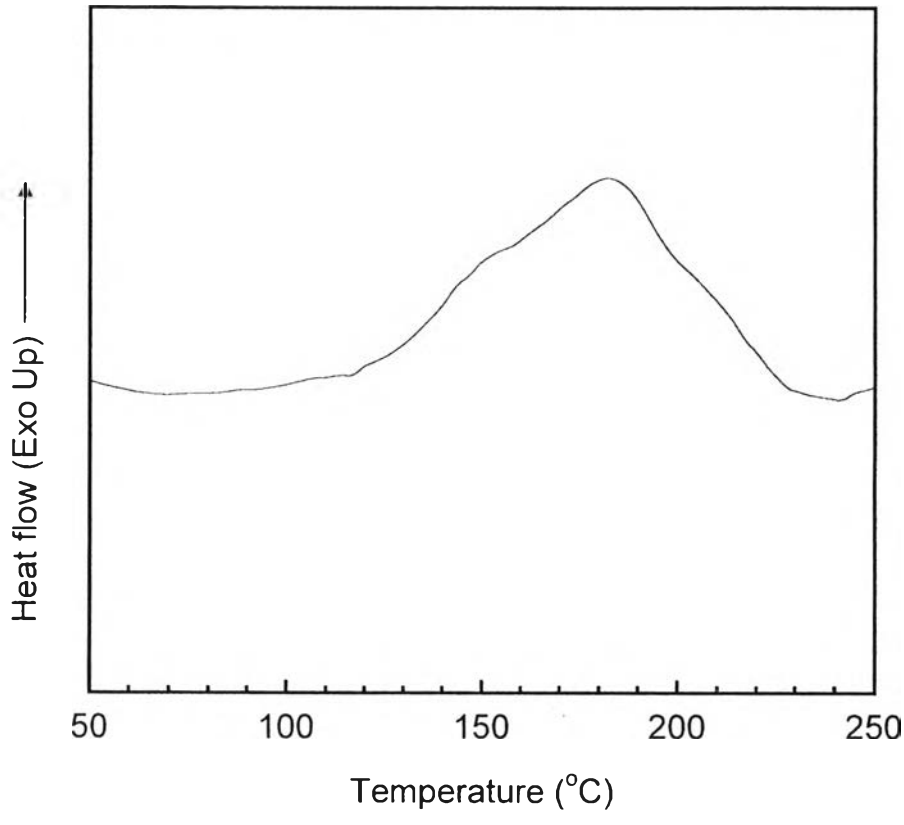

Figure 5.1 DSC thermogram of the benzoxazine monomer with scanning rate of 1 °C/min.

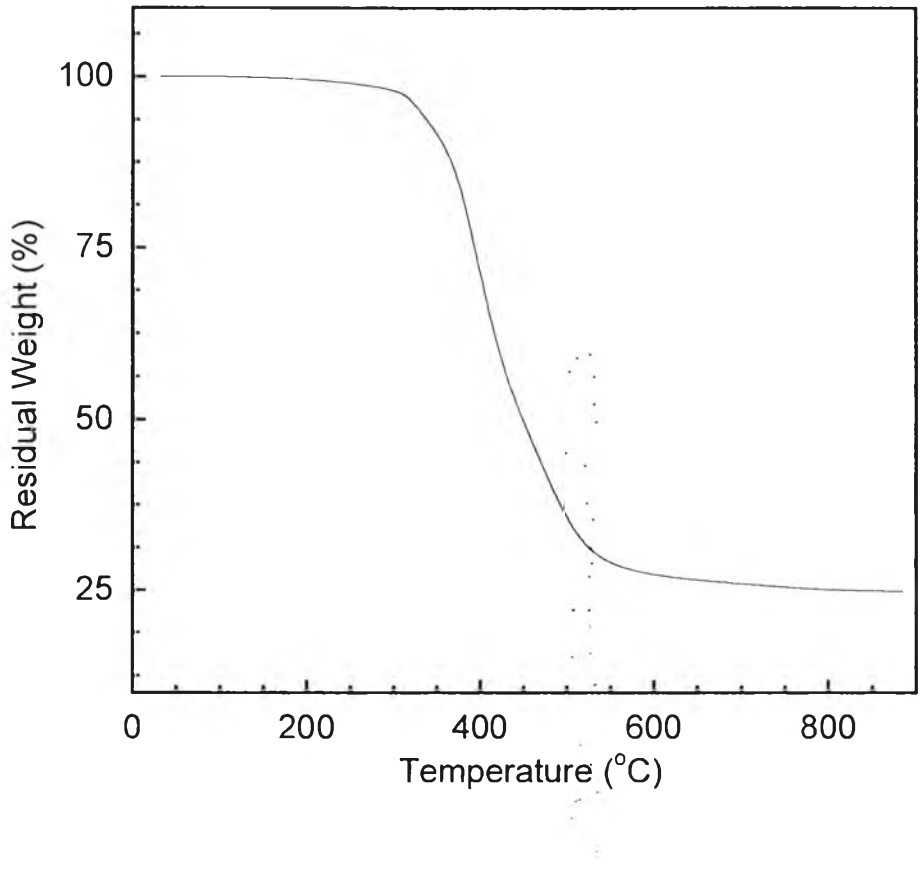

Figure 5.2 TGA thermogram of the polybenzoxazine.

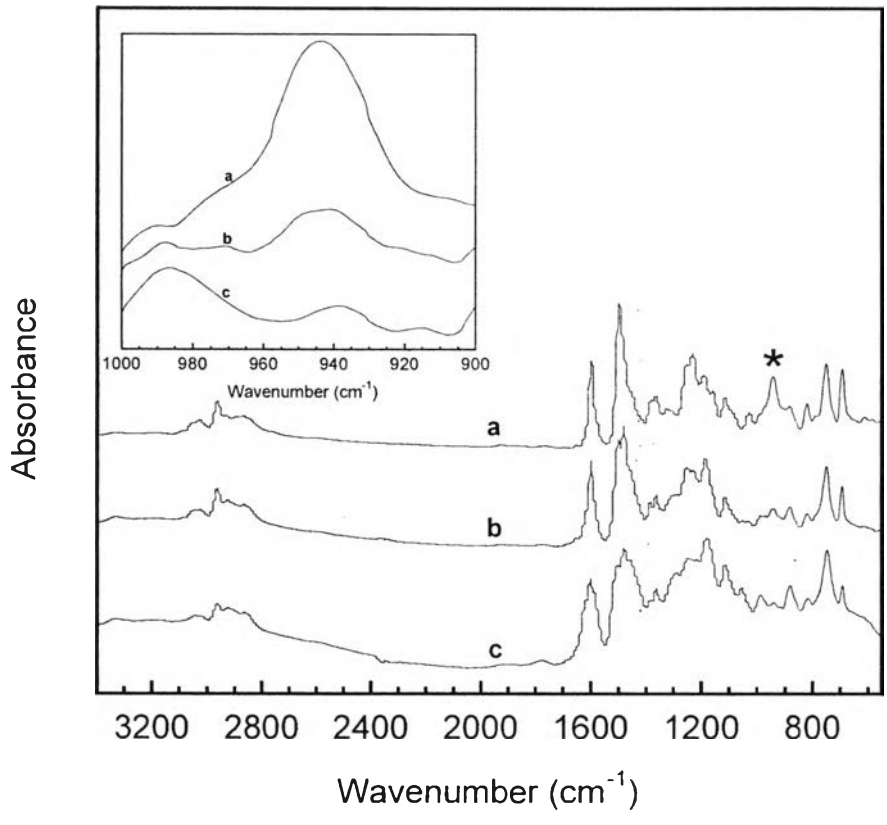

Figure 5.3 FTIR spectra of **a** benzoxazine monomer, **b** uncured BA-20% derived aerogel, and **c** uncured BA-40% derived aerogel.

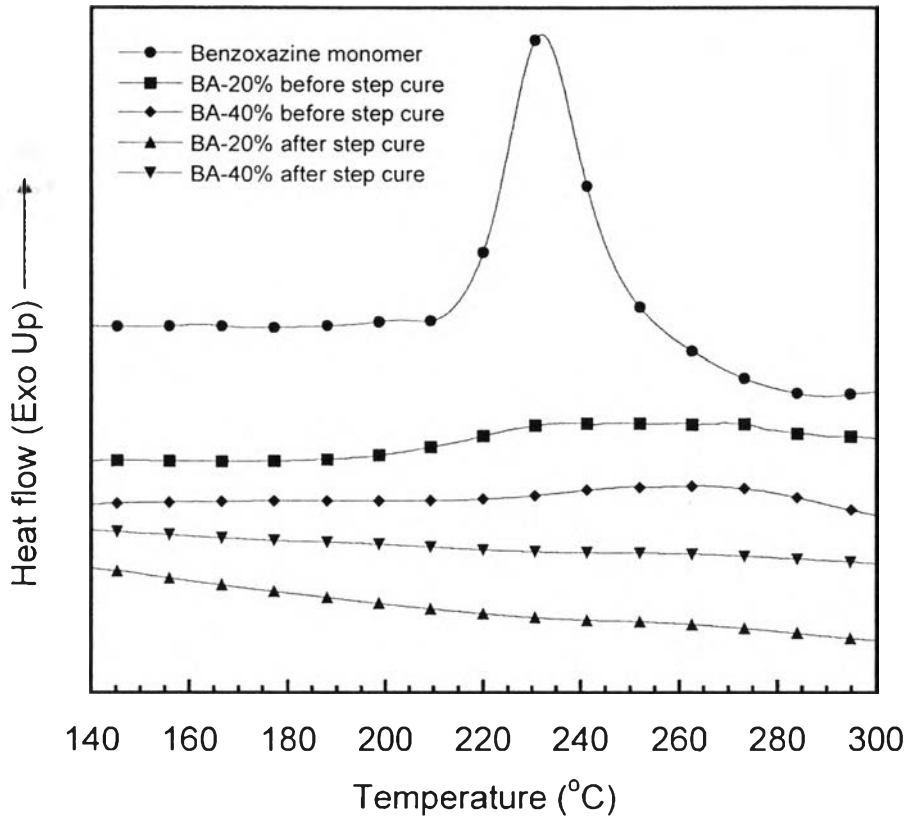

Figure 5.4 DSC thermograms of benzoxazine monomer, fully cured polybenzoxazine and polybenzoxazine aerogels.

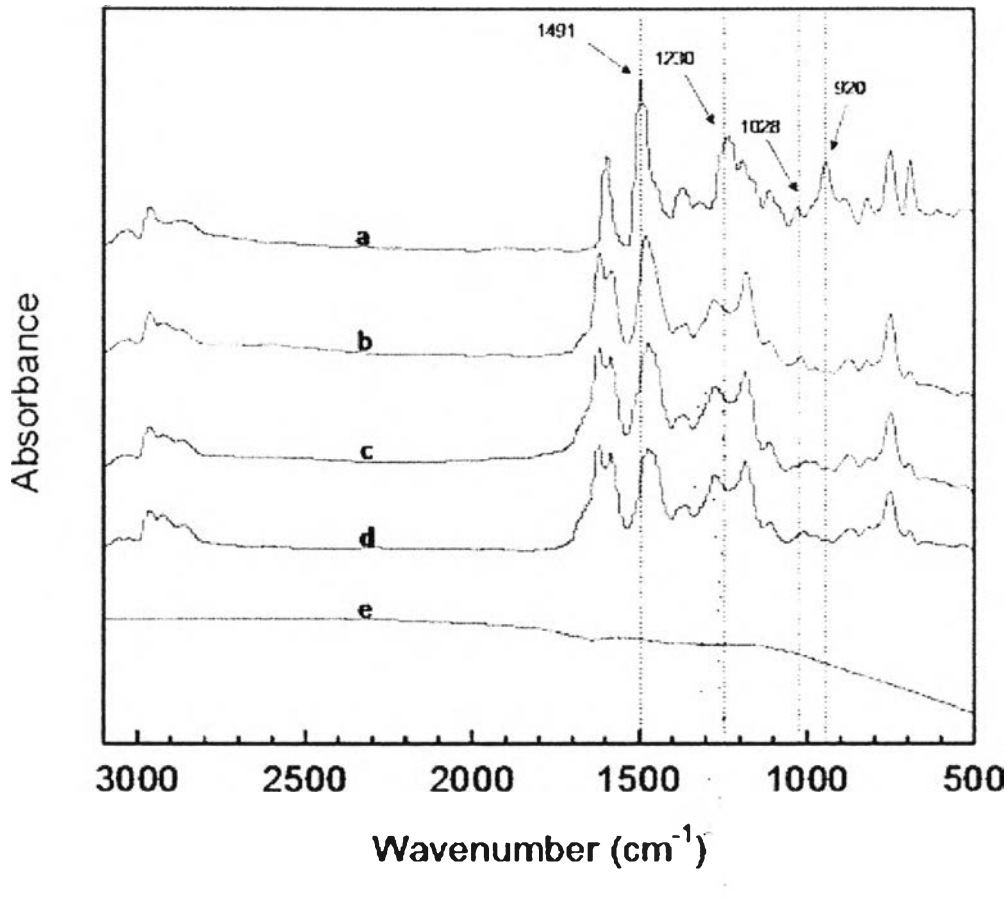

Figure 5.5 FTIR spectra of **a** benzoxazine monomer, **b** fully cured polybenzoxazine, **c** fully cured BA-20% derived aerogel, **d** fully cured BA-40% derived aerogel, **e** BA-40% derived carbon aerogel.

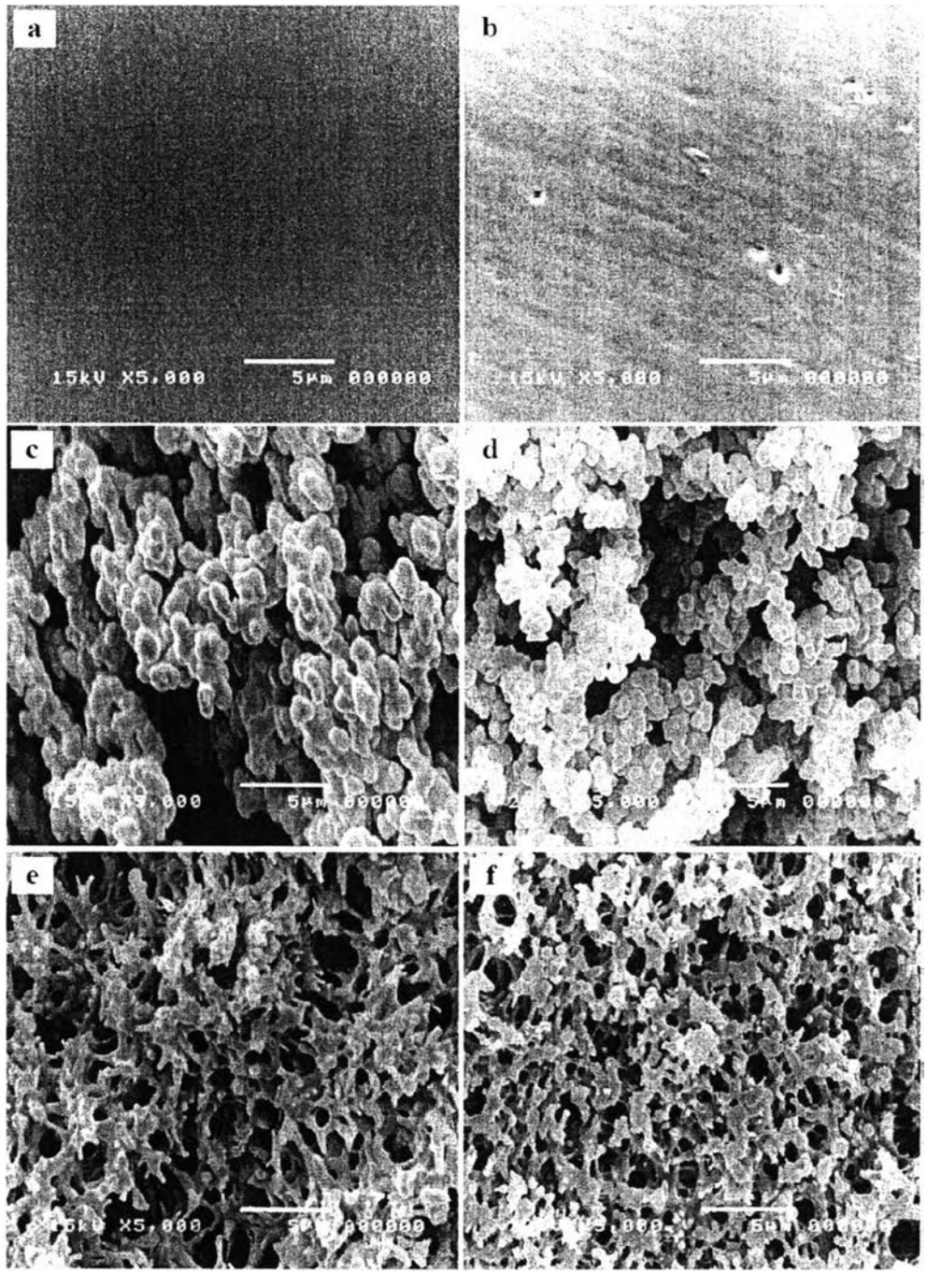

Figure 5.6 SEM micrographs of **a** fully cured polybenzoxazine, **b** carbonized polybenzoxazine, **c** fully cured organic aerogel from 20 wt% monomer solution, **d** carbon aerogel from 20 wt% monomer solution, **e** fully cured organic aerogel from 40 wt% monomer solution, and **f** carbon aerogel 40 wt% monomer solution.

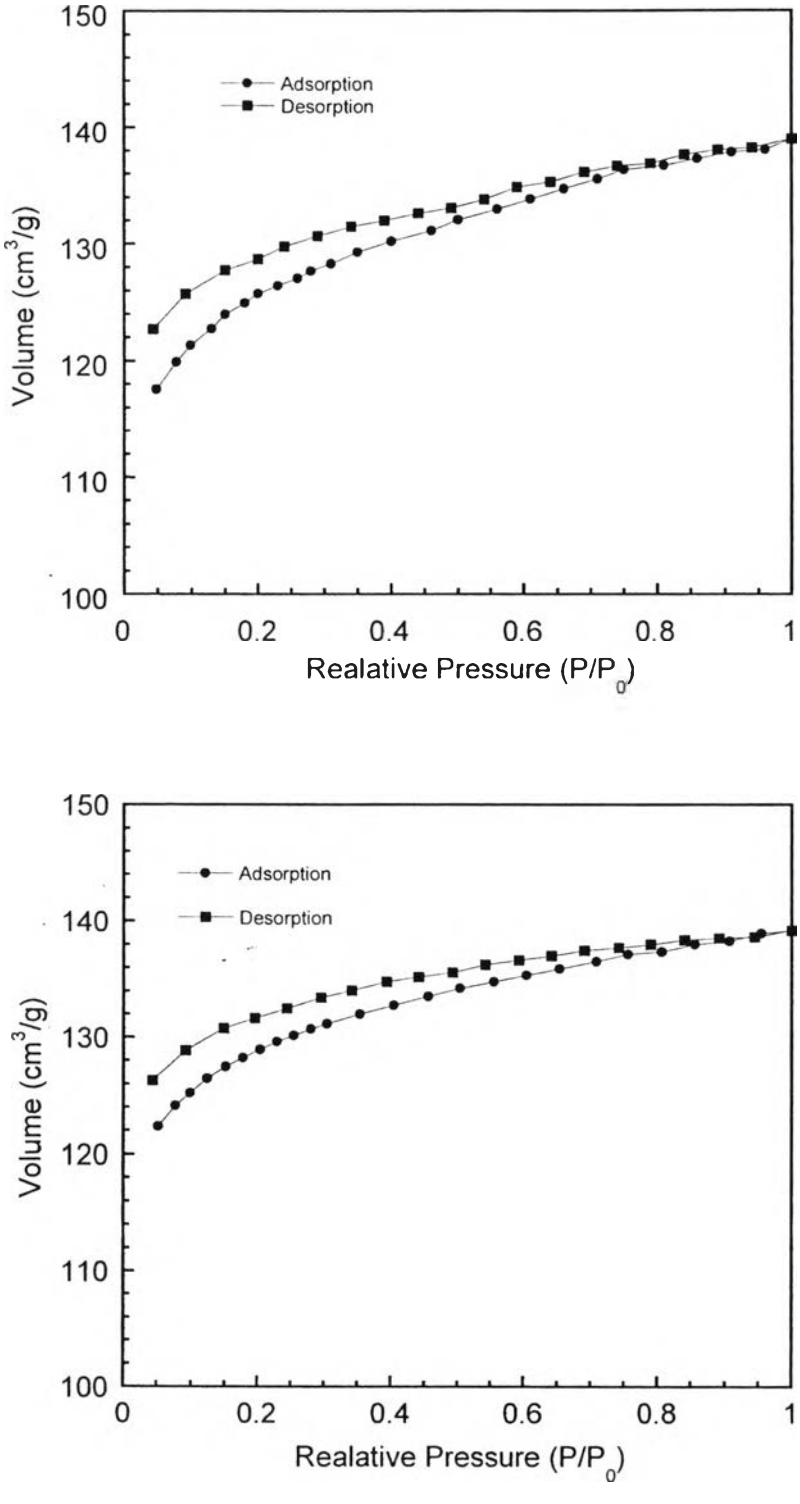

Figure 5.7 Adsorption and desorption isotherms of carbon aerogel from a 20 wt% monomer solution and b 40 wt% monomer solution.

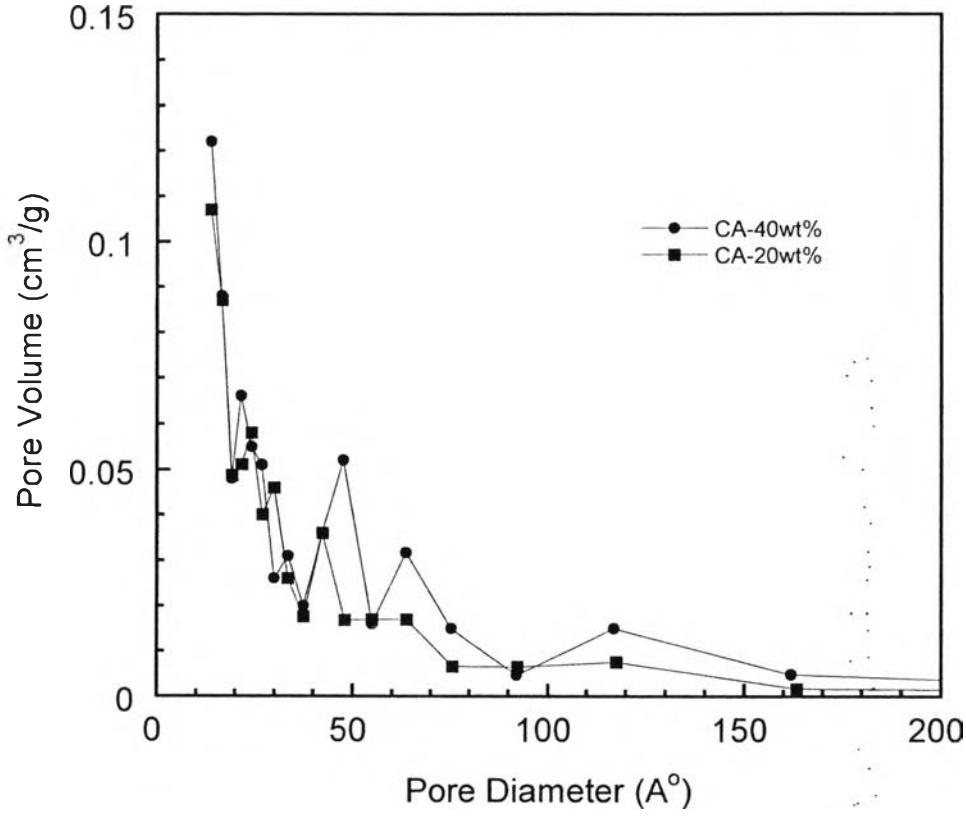

Figure 5.8 Pore size distribution of carbon aerogels from different monomer concentrations.

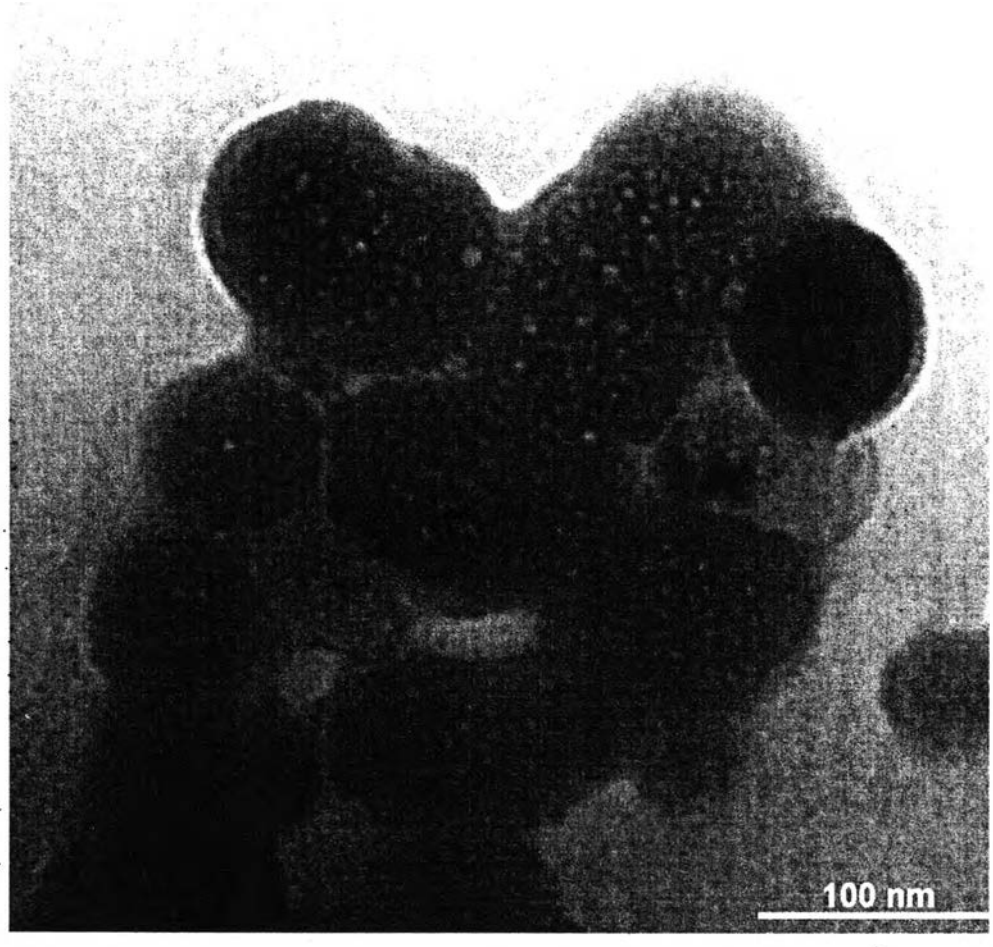

Figure 5.9 TEM morphology of carbon aerogel prepared from 40 wt% monomer solution.

Table 5.1 Density and pore texture of polybenzoxazine, polybenzoxazine aerogels and carbon aerogels

Sample	Density	S_{BET}	Total pore volume	Average pore size diameter	Volume shrinkage
	(kg/m^3)	(m^2/g)	(cm^3/g)	(nm)	(%)
Polybenzoxazine	1250	-	-	-	-
BA-20 wt%	260	-	-	-	-
BA-40 wt%	590	3.72	0.01	10.5	-
CA-20 wt%	300	384	0.21	2.2	53
CA-40 wt%	830	391	0.21	2.2	57

Table 5.2 The calculated surface area, pore volume and pore size of the resultant carbon aerogels compared with that of carbon aerogels from other organic precursors

Sample	Density (kg/m^3)	S_{mic} (m^2/g)	S_{mes} (m^2/g)	V_{mic} (cm^3/g)	V_{mes} (cm^3/g)	V_{mic}/V_{mes}	S_{mic}/S_{mes}
CA-20wt%	300	296	103	0.15	0.06	2.5	2.87
RF aerogel [1], Rf = 30wt%, R/F = 0.4 [12]	330	326	511	0.15	1.33	0.11	0.64
PF aerogel [2], PF = 50wt%, HCl /P = 1.5 [10]	320	229	297	0.11	0.71	0.15	0.77
PF aerogel [2], PF = 40wt%, NaOH = 0.01 wt% [11]	310	297	325	0.14	1.01	0.14	0.91
CA-40wt%	830	317	84	0.17	0.05	3.4	3.77
PF aerogel [2], PF = 70wt%, HCl /P = 3 [10]	640	326	192	0.15	0.51	0.29	1.70
PF aerogel [2], PF = 40wt%, NaOH = 0.07 wt% [11]	590	296	334	0.14	0.74	0.19	0.89
PF aerogel [2], PF = 60wt%, HCl /P = 3 [10]	510	359	206	0.17	0.67	0.25	1.74
RF aerogel [1], Rf = 40wt%, R/F = 0.33 [12]	500	304	528	0.14	1.09	0.13	0.58

RF aerogel[1] represents carbon aerogel from Resorcinol-Formaldehyde.
PF aerogel[2] represents carbon aerogel from Phenol-Furfural.